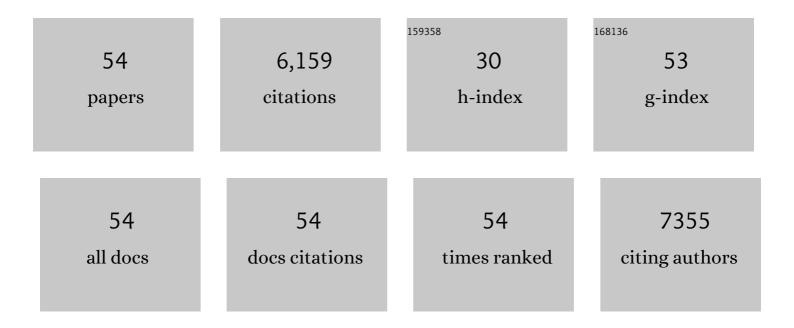
## Chih-Shan Tan

List of Publications by Year in descending order

Source: https://exaly.com/author-pdf/1937234/publications.pdf Version: 2024-02-01



#	Article	IF	CITATIONS
1	Accelerated discovery of CO2 electrocatalysts using active machine learning. Nature, 2020, 581, 178-183.	13.7	807
2	Molecular tuning of CO2-to-ethylene conversion. Nature, 2020, 577, 509-513.	13.7	682
3	Enhanced Nitrate-to-Ammonia Activity on Copper–Nickel Alloys via Tuning of Intermediate Adsorption. Journal of the American Chemical Society, 2020, 142, 5702-5708.	6.6	638
4	Copper nanocavities confine intermediates for efficient electrosynthesis of C3 alcohol fuels from carbon monoxide. Nature Catalysis, 2018, 1, 946-951.	16.1	354
5	Metal–Organic Frameworks Mediate Cu Coordination for Selective CO <sub>2</sub> Electroreduction. Journal of the American Chemical Society, 2018, 140, 11378-11386.	6.6	326
6	Catalyst synthesis under CO2 electroreduction favours faceting and promotes renewable fuels electrosynthesis. Nature Catalysis, 2020, 3, 98-106.	16.1	325
7	Perovskite seeding growth of formamidinium-lead-iodide-based perovskites for efficient and stable solar cells. Nature Communications, 2018, 9, 1607.	5.8	309
8	Copper-on-nitride enhances the stable electrosynthesis of multi-carbon products from CO2. Nature Communications, 2018, 9, 3828.	5.8	279
9	Lattice anchoring stabilizes solution-processed semiconductors. Nature, 2019, 570, 96-101.	13.7	208
10	Facet-Dependent Electrical Conductivity Properties of Cu <sub>2</sub> O Crystals. Nano Letters, 2015, 15, 2155-2160.	4.5	203
11	2D Metal Oxyhalideâ€Đerived Catalysts for Efficient CO <sub>2</sub> Electroreduction. Advanced Materials, 2018, 30, e1802858.	11.1	200
12	Efficient electrocatalytic conversion of carbon monoxide to propanol using fragmented copper. Nature Catalysis, 2019, 2, 251-258.	16.1	188
13	In Situ Back ontact Passivation Improves Photovoltage and Fill Factor in Perovskite Solar Cells. Advanced Materials, 2019, 31, e1807435.	11.1	143
14	Suppressed Ion Migration in Reduced-Dimensional Perovskites Improves Operating Stability. ACS Energy Letters, 2019, 4, 1521-1527.	8.8	130
15	Efficient upgrading of CO to C3 fuel using asymmetric C-C coupling active sites. Nature Communications, 2019, 10, 5186.	5.8	127
16	Chloride Passivation of ZnO Electrodes Improves Charge Extraction in Colloidal Quantum Dot Photovoltaics. Advanced Materials, 2017, 29, 1702350.	11.1	126
17	Strong Facet Effects on Interfacial Charge Transfer Revealed through the Examination of Photocatalytic Activities of Various Cu <sub>2</sub> O–ZnO Heterostructures. Advanced Functional Materials, 2017, 27, 1604635.	7.8	112
18	A Facet‧pecific Quantum Dot Passivation Strategy for Colloid Management and Efficient Infrared Photovoltaics. Advanced Materials, 2019, 31, e1805580.	11.1	87

CHIH-SHAN TAN

#	Article	IF	CITATIONS
19	Surface plasmon resonance enhancement of production of H2 from ammonia borane solution with tunable Cu2â^'xS nanowires decorated by Pd nanoparticles. Nano Energy, 2017, 31, 57-63.	8.2	65
20	Facet-Dependent Electrical Conductivity Properties of PbS Nanocrystals. Chemistry of Materials, 2016, 28, 1574-1580.	3.2	56
21	Contactless measurements of photocarrier transport properties in perovskite single crystals. Nature Communications, 2019, 10, 1591.	5.8	55
22	Facet-dependent optical properties of Pd–Cu <sub>2</sub> O core–shell nanocubes and octahedra. Nanoscale, 2015, 7, 11135-11141.	2.8	51
23	Enhanced Open ircuit Voltage in Colloidal Quantum Dot Photovoltaics via Reactivityâ€Controlled Solutionâ€Phase Ligand Exchange. Advanced Materials, 2017, 29, 1703627.	11.1	49
24	Metalâ€ŀike Band Structures of Ultrathin Si {111} and {112} Surface Layers Revealed through Density Functional Theory Calculations. Chemistry - A European Journal, 2017, 23, 11866-11871.	1.7	49
25	Facetâ€Ðependent Electrical Conductivity Properties of Silver Oxide Crystals. Chemistry - an Asian Journal, 2017, 12, 293-297.	1.7	48
26	Surfactant-Directed Fabrication of Supercrystals from the Assembly of Polyhedral Au–Pd Core–Shell Nanocrystals and Their Electrical and Optical Properties. Journal of the American Chemical Society, 2015, 137, 2265-2275.	6.6	47
27	Silicon Wafers with Facetâ€Dependent Electrical Conductivity Properties. Angewandte Chemie - International Edition, 2017, 56, 15339-15343.	7.2	46
28	Density Functional Theory Calculations Revealing Metalâ€like Band Structures for Ultrathin Germanium (111) and (211) Surface Layers. Chemistry - an Asian Journal, 2018, 13, 1972-1976.	1.7	41
29	Density Functional Theory Calculations Revealing Metalâ€like Band Structures and Work Function Variation for Ultrathin Gallium Arsenide (111) Surface Layers. Chemistry - an Asian Journal, 2019, 14, 2316-2321.	1.7	36
30	Polyhedral Cu2O to Cu pseudomorphic conversion for stereoselective alkyne semihydrogenation. Chemical Science, 2018, 9, 2517-2524.	3.7	34
31	Sequential Cation Exchange Generated Superlattice Nanowires Forming Multiple p–n Heterojunctions. ACS Nano, 2014, 8, 9422-9426.	7.3	29
32	Magnetic MoS <sub>2</sub> Interface Monolayer on a CdS Nanowire by Cation Exchange. Journal of Physical Chemistry C, 2016, 120, 23055-23060.	1.5	24
33	Strain Control of a NO Gas Sensor Based on Ga-Doped ZnO Epilayers. ACS Applied Electronic Materials, 2020, 2, 1365-1372.	2.0	24
34	Surface-dependent band structure variations and bond-level deviations in Cu <sub>2</sub> O. Inorganic Chemistry Frontiers, 2021, 8, 4200-4208.	3.0	24
35	Enhancement of perpendicular coercivity in L11 CoPt thin films by replacement of Co with Cu. Journal of Applied Physics, 2010, 108, 113909.	1.1	20
36	Facet-Dependent Surface Trap States and Carrier Lifetimes of Silicon. Nano Letters, 2020, 20, 1952-1958.	4.5	20

CHIH-SHAN TAN

#	Article	IF	CITATIONS
37	Current Rectification and Photo-Responsive Current Achieved through Interfacial Facet Control of Cu <sub>2</sub> O–Si Wafer Heterojunctions. ACS Central Science, 2021, 7, 1929-1937.	5.3	19
38	Reliability study on deep-ultraviolet photodetectors based on ZnGa2O4 epilayers grown by MOCVD. Applied Surface Science, 2021, 555, 149657.	3.1	18
39	Lattice‣ymmetryâ€Driven Epitaxy of Hierarchical GaN Nanotripods. Advanced Functional Materials, 2017, 27, 1604854.	7.8	17
40	Energy-Saving ZnGa <sub>2</sub> O <sub>4</sub> Phototransistor Improved by Thermal Annealing. ACS Applied Electronic Materials, 2020, 2, 3515-3521.	2.0	15
41	Large Facet-Specific Built-in Potential Differences Affecting Trap State Densities and Carrier Lifetimes of GaAs Wafers. Journal of Physical Chemistry C, 2020, 124, 21577-21582.	1.5	15
42	Germanium Possessing Facet-Specific Trap States and Carrier Lifetimes. Journal of Physical Chemistry C, 2020, 124, 13304-13309.	1.5	15
43	Heterogeneous Supersaturation in Mixed Perovskites. Advanced Science, 2020, 7, 1903166.	5.6	13
44	Silicon Wafers with Facetâ€Dependent Electrical Conductivity Properties. Angewandte Chemie, 2017, 129, 15541-15545.	1.6	12
45	Power Saving High Performance Deep-Ultraviolet Phototransistors Made of ZnGa <sub>2</sub> O <sub>4</sub> Epilayers. ACS Applied Electronic Materials, 2020, 2, 590-596.	2.0	10
46	Surface-dependent band structure variations and bond deviations of GaN. Physical Chemistry Chemical Physics, 2022, 24, 9135-9140.	1.3	10
47	Wearable Devices Made of a Wireless Vertical-Type Light-Emitting Diode Package on a Flexible Polyimide Substrate with a Conductive Layer. ACS Applied Electronic Materials, 2021, 3, 979-987.	2.0	9
48	Pentafluoropyridine functionalized novel heteroatom-doped with hierarchical porous 3D cross-linked graphene for supercapacitor applications. RSC Advances, 2021, 11, 26892-26907.	1.7	8
49	Lead-Free Ultra-Wide Direct Bandgap Perovskite EACal <sub>3</sub> . IEEE Nanotechnology Magazine, 2022, 21, 66-70.	1.1	8
50	Density Functional Theory Study of Metallic Silicon (111) Plane Structures. ACS Omega, 2022, 7, 5385-5392.	1.6	8
51	Transition Metal lons in Methylammonium Chloride Perovskites. ACS Omega, 2022, 7, 1412-1419.	1.6	7
52	Intermediates in the cation reactions in solution probed by an in situ surface enhanced Raman scattering method. Scientific Reports, 2015, 5, 13759.	1.6	6
53	Optoelectronic Properties Prediction of Lead-Free Methylammonium Alkaline-Earth Perovskite Based on DFT Calculations. ACS Omega, 2022, 7, 16204-16210.	1.6	6
54	Synthesis, characterization, and band gap tunability in Ternary Zn <inf>x</inf> Cd <inf>1−x</inf> S (0 ≤ x ≤ 1) alloyed nanowires. , 2014, , .		1